

Online Research @ Cardiff

This is an Open Access document downloaded from ORCA, Cardiff University's institutional repository: <https://orca.cardiff.ac.uk/id/eprint/98114/>

This is the author's version of a work that was submitted to / accepted for publication.

Citation for final published version:

Khoj, Manal A, Hughes, Colan Evan, Harris, Kenneth David Maclean ORCID: <https://orcid.org/0000-0001-7855-8598> and Kariuki, Benson ORCID: <https://orcid.org/0000-0002-8658-3897> 2017. Structural diversity of solid solutions formed between 3-chloro-trans-cinnamic acid and 3-bromo-trans-cinnamic acid. *Crystal Growth and Design* 17 (3) , pp. 1276-1284. 10.1021/acs.cgd.6b01675 file

Publishers page: <http://dx.doi.org/10.1021/acs.cgd.6b01675>
<<http://dx.doi.org/10.1021/acs.cgd.6b01675>>

Please note:

Changes made as a result of publishing processes such as copy-editing, formatting and page numbers may not be reflected in this version. For the definitive version of this publication, please refer to the published source. You are advised to consult the publisher's version if you wish to cite this paper.

This version is being made available in accordance with publisher policies.

See

<http://orca.cf.ac.uk/policies.html> for usage policies. Copyright and moral rights for publications made available in ORCA are retained by the copyright holders.



Structural diversity of solid solutions formed between 3-chloro-trans-cinnamic acid and 3-bromo-trans-cinnamic acid

Manal A. Khoj, Colan E. Hughes, Kenneth D.M. Harris, and Benson M. Kariuki

Crystal Growth and Design

Structural diversity of solid solutions formed between 3-chloro-*TRANS*-cinnamic acid and 3-bromo-*TRANS*-cinnamic acid

Manal A. Khoj, Colan E. Hughes, Kenneth D. M. Harris* and Benson M. Kariuki*

School of Chemistry, Cardiff University, Main Building, Park Place, Cardiff, CF10 3AT, U.K.

Authors for correspondence, e-mails: KariukiB@cardiff.ac.uk; HarrisKDM@cardiff.ac.uk

Abstract

The formation and structural properties of solid solutions containing 3-chloro-*trans*-cinnamic acid (3-CICA) and 3-bromo-*trans*-cinnamic acid (3-BrCA) are explored across a range of compositions. Two distinct γ -type structures of 3-CICA/3-BrCA solid solutions and two distinct β -type structures of 3-CICA/3-BrCA solid solutions are reported and structurally characterized. One of the γ -type structures is isostructural with the known γ polymorphs of pure 3-CICA and pure 3-BrCA, whereas the other γ -type structure has not been observed previously for either pure 3-CICA or pure 3-BrCA (representing a rare case in which the structure of the solid solution is not known for the pure phases of either of the constituent molecules). One of the β -type structures of the 3-CICA/3-BrCA solid solutions is similar to the β polymorph of pure 3-CICA, whereas the other β -type structure is similar to the β polymorph of pure 3-BrCA. The specific β -type structure formed is found to depend on the relative amounts of 3-BrCA and 3-CICA in the solid solution. UV irradiation of the β -type 3-CICA/3-BrCA solid solution with 1:1 composition yields three different photodimers, with substituents {Cl,Cl}, {Cl,Br} or {Br,Br} in the approximate ratio 1:2:1 respectively, consistent with the occurrence of a topochemical reaction in a solid solution with a random distribution of 3-CICA and 3-BrCA molecules.

Introduction

Organic solid-state chemistry has significant (but under-exploited) potential applications as a method in organic synthesis, through the controlled aggregation of reactant molecules in the solid-state by crystal engineering strategies, and then carrying out a solid-state chemical transformation to generate a targeted product. The main advantages of solid-state reactions over fluid state reactions emanate from the relatively more restricted reaction environment, which leads in many cases to high selectivity, novel products, stereochemically pure products and high efficiency.

The outcome of many solid-state reactions can be predicted on the basis of the topochemical principle,¹⁻¹⁶ according to which the reaction pathway (and hence the specific product obtained) is controlled by the spatial arrangement of molecules in the reactant crystal structure.³ *Trans*-cinnamic acid and its derivatives played a historically significant role in rationalizing the relationships between the structure and properties of crystalline organic solids,^{3,4} particularly with regard to photochemical reactivity. On the basis of their behaviour in [2+2] photodimerization reactions,^{3,17} crystalline *trans*-cinnamic acids may be categorized into three classes, denoted α , β and γ . On UV irradiation, α -type crystals produce a centrosymmetric (α -truxillic acid) dimer, β -type crystals produce a mirror-symmetric (β -truxinic acid) dimer, whereas no reaction occurs on UV irradiation of γ -type crystals.

Clear correlations have been established between the crystal structures, determined from single-crystal X-ray diffraction (XRD), and the photoreactivity of these materials.^{3,4,8} Each of the α , β and γ types of crystal has a distinct mode of molecular packing. For photoreactive crystals (i.e., α -type and β -type), the distance between the centres of the C=C bonds of potentially reactive monomer molecules is less than *ca.* 4.2 Å, whereas the corresponding distance for the photostable γ -type crystals is greater than *ca.* 4.7 Å. The distinction between the crystal structures of the photoreactive α -type and β -type crystals is that photoreactive monomer molecules are related across a crystallographic inversion centre in the α -type structures (leading to a centrosymmetric dimer molecule) whereas photoreactive monomer molecules are related by translation in the β -type structures (leading to a mirror-symmetric dimer molecule).

1
2
3
4
5
6
7
8
9
10
11
12
13
14
15
16
17
18
19
20
21
22
23
24
25
26
27
28
29
30
31
32
33
34
35
36
37
38
39
40
41
42
43
44
45
46
47
48
49
50
51
52
53
54
55
56
57
58
59
60

Thus, from knowledge of the topochemical principle, it is clear why specific stereoisomers of α -truxillic acids (from photodimerization of α -type *trans*-cinnamic acids) and β -truxinic acids (from photodimerization of β -type *trans*-cinnamic acids) are produced in these solid-state reactions. However, synthesis of unsymmetrical products, resulting from two different *trans*-cinnamic acid derivatives undergoing photodimerization, is a greater challenge. Nevertheless, such molecules can be obtained by solid-state reactions through the application of crystal engineering principles, as exemplified by the synthesis of 3-(3',5'-dinitrophenyl)-4-(2,5'-dimethoxyphenyl)-cyclobutane-1,2-dicarboxylic acid from a stoichiometric co-crystal of the two reactant molecules prearranged through donor-acceptor interactions.^{18,19} An alternative approach to the solid-state synthesis of unsymmetric molecules is through the formation of solid solutions utilizing materials that are already known to crystallize with an appropriate crystal structure to give rise to a topochemical solid-state reaction.²⁰⁻²⁴ The use of a third component in the crystal to organize the reactants in a solid solution has also been elegantly demonstrated.²⁵

In the present paper, we report the formation and structural characterization of solid solutions containing 3-chloro-*trans*-cinnamic acid (denoted 3-CICA) and 3-bromo-*trans*-cinnamic acid (denoted 3-BrCA). We also investigate the photochemical behaviour of one of the solid solutions prepared in this work. The molecular structures of 3-CICA and 3-BrCA are shown in Scheme 1. The preparation procedures that have been found to produce structurally distinct solid solutions of 3-CICA and 3-BrCA are summarized in Table 1.

For pure 3-CICA, the crystal structures of a β -type polymorph²⁶ and a γ -type polymorph²⁷ have been reported, while for pure 3-BrCA, the crystal structures of a β -type polymorph²⁶ and a γ -type polymorph²⁸ have also been reported. The β polymorphs of pure 3-CICA and pure 3-BrCA are structurally different, whereas the γ polymorphs of pure 3-CICA and pure 3-BrCA are isostructural (see Table 2). Recognizing that the γ polymorphs of pure 3-CICA and pure 3-BrCA are isostructural led us to anticipate that the formation of solid solutions of 3-CICA and 3-BrCA may be possible.

Results and Discussion

Structural Classification

The solid solutions of 3-CICA and 3-BrCA discussed in this paper are denoted 3-(Cl/Br)CA, and the composition of each solid solution is specified as the mole fraction of 3-CICA (denoted x_{Cl}). Among the four different crystalline forms of 3-(Cl/Br)CA solid solutions found in this work, two forms have β -type structures and two forms have γ -type structures.

The β polymorphs of pure 3-CICA and pure 3-BrCA have different crystal structures (while both conforming to the β -type classification), which we denote as $\beta^{(Cl)}$ and $\beta^{(Br)}$ respectively. The two β -type forms of the 3-(Cl/Br)CA solid solutions reported below correspond to the $\beta^{(Cl)}$ and $\beta^{(Br)}$ structure types (but with disorder of the Cl/Br substituents).

In contrast, the γ polymorph of pure 3-CICA and the γ polymorph of pure 3-BrCA are isostructural. One of the γ -type forms of the 3-(Cl/Br)CA solid solutions reported here corresponds to the structure of the γ polymorphs of pure 3-CICA and pure 3-BrCA, and is denoted the γ form of the 3-(Cl/Br)CA solid solutions. The other γ -type form of the 3-(Cl/Br)CA solid solutions represents a new structure (different from the γ polymorphs of pure 3-CICA and pure 3-BrCA) and this new structure type is denoted the γ' form of the 3-(Cl/Br)CA solid solutions.

In all four structure types (i.e., $\beta^{(Cl)}$, $\beta^{(Br)}$, γ and γ') observed for the 3-(Cl/Br)CA solid solutions, the 3-CICA and 3-BrCA molecules are planar. However, for planar molecules of 3-CICA and 3-BrCA, there are two possible conformations labelled *syn* and *anti* in Scheme 1. The $\beta^{(Cl)}$, γ and γ' structure types all contain molecules in the *anti* conformation, whereas the $\beta^{(Br)}$ structure type contains molecules in the *syn* conformation. We note that the γ polymorphs of pure 3-CICA and pure 3-BrCA contain the *anti* conformation, the β polymorph of pure 3-CICA also contains the *anti* conformation, and the β polymorph of pure 3-BrCA contains the *syn* conformation.

3-(Cl/Br)CA Solid Solutions with the γ and γ' Structure Types

As noted above, crystallization of 3-CICA and 3-BrCA was found to give 3-(Cl/Br)CA solid solutions (see Table 1) with two different γ -type structures, denoted γ and γ' . The γ form of the

1
2
3 3-(Cl/Br)CA solid solutions was obtained by crystallization from a solution containing 3-ClCA
4 and 3-BrCA (1:1 molar ratio) in methanol. The powder XRD pattern of the material obtained was
5 very similar to those of the γ polymorphs of pure 3-ClCA and pure 3-BrCA, but with peak
6 positions that are indicative of unit cell dimensions intermediate between the two pure phases.
7
8 Single-crystal XRD confirmed that the structure of the solid solution is monoclinic ($P2_1/a$) and
9 isostructural with the γ forms of pure 3-ClCA²⁶ and pure 3-BrCA²⁸ and 3-methylcinnamic acid²⁹.
10
11 Crystallographic data are shown in Table 3 and the crystal structure is shown in Fig. 1. The
12 asymmetric unit comprises one “average” molecule of 3-(Cl/Br)CA, with the Cl/Br site
13 disordered. For the specific crystal studied, the refined occupancies for the Cl/Br site were 0.56(1)
14 for Cl and 0.44(1) for Br, corresponding to $x_{Cl} = 0.56$. The crystal structure (as described
15 previously for pure 3-ClCA²⁶ and pure 3-BrCA²⁸) consists of hydrogen-bonded carboxylic acid
16 dimers stacked along the b -axis (Fig. 1a). These stacks form layers parallel to the (102^-) plane
17 (alternating layers are displayed as red and blue molecules in Fig. 1). Within a given layer, the
18 stacks of hydrogen-bonded dimers are arranged in a “herringbone” type of pattern (Fig 1b).
19
20
21
22
23
24
25
26
27
28
29

30 Crystallization of 3-ClCA and 3-BrCA (in 1:1 molar ratio) from acetone gave a mixture of plate-
31 like and needle-like crystals. By a combination of powder and single-crystal XRD analysis, the plate
32 like crystals were confirmed to be the γ form of the 3-(Cl/Br)CA solid solution discussed above,
33 whereas the needle-like crystals represented a new solid phase. The crystal structure (Fig. 2) of the
34 new phase was determined by single-crystal XRD to a monoclinic (space group $P2_1/n$) γ -type
35 structure containing one “averaged” 3-(Cl/Br)CA molecule in the asymmetric unit, with disorder of
36 the Cl/Br substituent. For the specific crystal studied, the refined occupancies were 0.61(1) for Cl and
37 0.39(1) for Br. This structure is denoted the γ' form of the 3-(Cl/Br)CA solid solutions.
38
39
40
41
42
43
44
45

46 In the crystal structure of the γ' form of the 3-(Cl/Br)CA solid solutions (Fig. 2a), hydrogen-
47 bonded carboxylic acid dimers are stacked along the a -axis. The distance between the centres of
48 adjacent C=C bonds is 4.967Å, consistent with their assignment to the γ -type classification.
49
50 Adjacent stacks are related by translation along the c -axis, giving rise to two-dimensional arrays
51 (“slabs”) of molecules parallel to the ac -plane. As the halogen atoms protrude from the surfaces
52 of these slabs, the interface between adjacent slabs is dominated by van-der Waals interactions
53 between halogen atoms.
54
55
56
57
58
59
60

1
2
3
4
5
6
7
8
9
10
11
12
13
14
15
16
17
18
19
20
21
22
23
24
25
26
27
28
29
30
31
32
33
34
35
36
37
38
39
40
41
42
43
44
45
46
47
48
49
50
51
52
53
54
55
56
57
58
59
60

In the crystals of the γ and γ' forms studied by single-crystal XRD, the mole fraction of 3-CICA was $x_{Cl} \approx 0.6$, while the mole fraction in the crystallization solution was $x_{Cl} = 0.5$. This observation suggests that there is preferential uptake of 3-CICA within the γ and γ' forms of the 3-(Cl/Br)CA solid solutions, possibly reflecting differences in solubility between 3-CICA and 3-BrCA under the conditions of the crystallization experiment.

We note that the γ' form of the 3-(Cl/Br)CA solid solutions is an interesting case in which the structure type found for a solid solution is not known for the pure phases of either of the constituent molecules.

3-(Cl/Br)CA Solid Solutions with the $\beta^{(Cl)}$ and $\beta^{(Br)}$ Structure Types

Initially, crystallization from the molten phase was investigated, starting from a physical mixture of 3-CICA and 3-BrCA with 1:1 molar ratio (see Experimental section). The powder XRD pattern of the material obtained following crystallization from the melt is similar to that of the β polymorph of pure 3-BrCA, but with peaks shifted to slightly higher 2θ values. This observation is consistent with the formation of a solid solution of 3-BrCA and 3-CICA in the structure type of the β polymorph of pure 3-BrCA (the shifts of peaks to slightly higher 2θ values arise because 3-CICA has a lower molecular volume than 3-BrCA, leading to a slightly contracted unit cell in the solid solution in accordance with Vegard's Law^{30,31}). We note that, in the case of samples prepared from the molten mixture, the overall composition of the solid solution is expected to be very close to the composition of the initial physical mixture of 3-CICA and 3-BrCA used.

The same procedure was followed to prepare 3-(Cl/Br)CA solid solutions from the molten phase starting from physical mixtures of 3-CICA and 3-BrCA with molar ratios corresponding to the following mole fractions of 3-CICA: $x_{Cl} = 0.17, 0.25, 0.33, 0.67, 0.75, 0.80, 0.83$. The powder XRD patterns (Fig. 3) for the 3-(Cl/Br)CA solid solutions prepared with composition in the range $x_{Cl} = 0.17 - 0.67$ are essentially the same as that (with slight shifts in peak positions) for the β polymorph of pure 3-BrCA²⁶ (i.e., $x_{Cl} = 0$; see Table 2). This structure type of the 3-(Cl/Br)CA solid solutions is denoted $\beta^{(Br)}$. For the 3-(Cl/Br)CA solid solutions prepared from physical mixtures with mole fraction of 3-CICA in the range $x_{Cl} = 0.75 - 0.83$, the powder XRD pattern is similar to that for the β polymorph of pure 3-CICA²⁶ (i.e., $x_{Cl} = 1$; see Table 2), again with a slight shift in peak

1
2 positions consistent with the formation of solid solutions. This structure type of the 3-(Cl/Br)CA
3 solid solutions is denoted $\beta^{(\text{Cl})}$.
4
5

6
7 Thus, depending on the composition of the 3-(Cl/Br)CA solid solutions, either the $\beta^{(\text{Cl})}$
8 structure type or the $\beta^{(\text{Br})}$ structure type is formed. The change in structure type occurs at a critical
9 composition corresponding to mole fraction of 3-ClCA in the molten precursor phase in the
10 region of $x_{\text{Cl}} \approx 0.67 - 0.75$.
11
12
13

14
15 In DSC data recorded for these 3-(Cl/Br)CA solid solutions (Fig. 4), the melting endotherm is
16 consistent with an essentially monophasic sample. Across the composition range starting from x_{Cl}
17 = 0 (pure 3-BrCA), the onset temperature decreases monotonically as the amount of 3-ClCA in
18 the solid solution is increased, consistent with the formation of a solid solution. A discontinuity in
19 behaviour is observed when the mole fraction of 3-ClCA is in the region $x_{\text{Cl}} = 0.75 - 0.80$, close
20 to the composition at which the crystal structure of the solid solutions changes from the $\beta^{(\text{Br})}$
21 structure type to the $\beta^{(\text{Cl})}$ structure type.
22
23
24
25
26
27
28
29

30 *Structural Properties of the $\beta^{(\text{Br})}$ Form of 3-(Cl/Br)CA Solid Solutions*

31
32

33 The $\beta^{(\text{Br})}$ form of the 3-(Cl/Br)CA solid solutions was also obtained by crystallization from
34 a solution containing 3-ClCA and 3-BrCA in 1:1 molar ratio in glacial acetic acid. The powder
35 XRD pattern of the product is identical to that of the material with 1:1 molar ratio prepared by
36 crystallization from the molten phase, indicating that the solid form obtained is $\beta^{(\text{Br})}$. The crystal
37 structure of the $\beta^{(\text{Br})}$ form was determined using a crystal obtained from the solution-state
38 crystallization.
39
40
41
42
43
44

45 The crystal structure of the $\beta^{(\text{Br})}$ form of the 3-(Cl/Br)CA solid solutions (Fig. 5a) is monoclinic
46 with space group C2/c. The asymmetric unit comprises one “average” molecule of 3-(Cl/Br)CA, with
47 disorder at the Cl/Br site. The structure comprises hydrogen-bonded carboxylic acid dimers stacked
48 along the *b*-axis. The distance between the centres of adjacent C=C bonds along the stack is 3.865 Å,
49 consistent with a photoreactive β -type structure. These stacks form layers parallel to the (1⁻02) plane
50 and, within a given layer, the stacks of hydrogen-bonded dimers are arranged in a “herringbone”
51 type of pattern (Fig. 5b). In many respects, this structure is
52
53
54
55
56
57
58
59
60

1
2
3 reminiscent of the γ polymorphs of 3-ClCA and 3-BrCA (except, of course, in terms of the
4 relation between adjacent molecules along the stack, such that the $\beta^{(\text{Br})}$ structure is photoreactive
5 and the γ polymorphs of 3-ClCA and 3-BrCA are photostable). For the specific crystal of the $\beta^{(\text{Br})}$
6 form of the 3-(Cl/Br)CA solid solutions studied, the refined occupancies were 0.510(4) for Cl and
7 0.490(4) for Br. Thus, in contrast to the situation noted above for the γ and γ' forms of 3-
8 (Cl/Br)CA solid solutions, the molar ratio of 3-ClCA to 3-BrCA in the $\beta^{(\text{Br})}$ solid solution
9 obtained from solution-state crystallization (glacial acetic acid) is essentially the same in the
10 crystal structure and in the crystallization solution (i.e., $x_{\text{Cl}} \approx 0.5$ for the crystal of the $\beta^{(\text{Br})}$ form
11 obtained from a solution with 1:1 molar ratio of 3-ClCA to 3-BrCA).
12
13
14
15
16
17
18
19

20 *Solid-State Photoreactivity of the $\beta^{(\text{Br})}$ Form of the 3-(Cl/Br)CA Solid Solutions*

21
22
23
24 Our studies of solid-state photoreactivity in the present work are focused on the 3-
25 (Cl/Br)CA solid solution with the $\beta^{(\text{Br})}$ structure type and composition $x_{\text{Cl}} \approx 0.5$ obtained from
26 solution-state crystallization. In the crystal structure of the $\beta^{(\text{Br})}$ form, potentially reactive
27 molecules are related by translation along the b -axis and the C=C bonds are parallel with a centre-
28 to-centre separation of 3.865 Å, corresponding to the ideal geometric arrangement for a solid-state
29 [2+2] photodimerization reaction in accordance with the topochemical principle.¹⁻¹⁶ Clearly, the
30 product distribution obtained in the photodimerization reaction provides direct insights
31 concerning the distribution of the 3-ClCA and 3-BrCA molecules within the crystalline solid
32 solution. In particular, if the material comprises large homo-molecular domains of 3-ClCA and
33 large homo-molecular domains of 3-BrCA, the products from topochemical photodimerization
34 would be predominantly 3,3'-dichloro- β -truxinic acid and 3,3'-dibromo- β -truxinic acid. However,
35 a completely random distribution of the two molecular components in the solid solution would
36 produce the three products 3,3'-dichloro- β -truxinic acid, 3-bromo-3'-chloro- β -truxinic acid and
37 3,3'-dibromo- β -truxinic acid in the ratio 1:2:1.
38
39
40
41
42
43
44
45
46
47
48
49
50

51
52 A powder sample of the $\beta^{(\text{Br})}$ form of the 3-(Cl/Br)CA solid solution was subjected to UV
53 irradiation and the occurrence of a reaction was evident from changes in the powder XRD data for
54 samples extracted periodically during the UV irradiation (see Experimental section). The powder
55 XRD data indicates that UV irradiation is associated with loss of crystallinity of the material (as
56
57
58
59
60

1
2
3 observed also for 3-fluorocinnamic acid³²). To monitor the progress of the reaction, IR spectra
4 were recorded every 12 hr over a period of 60 hr (Fig. 6). The intensity of the band at *ca.* 1629
5 cm^{-1} due to the C=C stretching mode decreases gradually as a function of irradiation time,
6
7 indicating a decrease in the amount of C=C bonds present as a result of the photodimerization
8
9 reaction. The shift in the C=O stretching band (band 1; from *ca.* 1670 cm^{-1} to *ca.* 1695 cm^{-1})
10
11 may be associated with loss of conjugation on dimerization.
12
13

14
15 Solution-state ^1H NMR spectra (Fig. 7a) were recorded for samples of the reaction product
16
17 extracted periodically during the UV irradiation and were fully consistent with the occurrence of the
18
19 photodimerization reaction. The intensity of the ^1H NMR peaks for the hydrogen atoms attached to
20
21 the carbon atoms of the C=C bond (*ca.* 6.8 ppm and 8.0 ppm; labelled 1 in Fig. 7a) in the reactant
22
23 molecules (unresolved for 3-ClCA and 3-BrCA) decreases as a function of irradiation time, whereas
24
25 the intensity of the ^1H NMR peaks for the hydrogen atoms of the cyclobutane moiety of the
26
27 photoproduct (*ca.* 4.1 and 4.8 ppm; labelled 2 Fig. 7a) increases as a function of irradiation time. The
28
29 solution-state ^1H NMR data indicate that over 95% of the molecules in the reactant phase were
30
31 converted in the reaction, and a plot of $\log_{10}(\text{reactant}\%)$ versus time (Fig. 7b) is linear (with
32
33 $R^2 = 0.995$), indicating first order kinetics.
34

35
36 Crystallization of the photoproduct followed by structure determination of the resultant
37
38 crystals would not necessarily provide conclusive proof that the 3-bromo-3'-chloro- β -truxinic acid
39
40 heterodimer is present in the reaction product, as 3,3'-dichloro- β -truxinic acid and 3,3'-dibromo- β -
41
42 truxinic acid homodimers are also produced. Clearly, 3,3'-dichloro- β -truxinic acid and 3,3'-
43
44 dibromo- β -truxinic acid could form a crystalline solid solution for which the *average* crystal
45
46 structure determined by diffraction techniques may be indistinguishable from the 3-bromo-3'-
47
48 chloro- β -truxinic acid heterodimer (i.e., the *average* crystal structure may be the same in each
49
50 case). However, the three different types of product molecule may be distinguished by mass
51
52 spectrometry and HPLC. The ES mass spectrum of the product sampled after 60 hr of UV
53
54 irradiation is consistent with the presence of the three different product molecules, with peaks due
55
56 to 3,3'-dichloro- β -truxinic acid and 3,3'-dibromo- β -truxinic acid homodimers observed at $m/z =$
57
58 363.03 and 452.94 respectively, and a peak due to the 3-bromo-3'-chloro- β -truxinic acid
59
60 heterodimer observed at $m/z = 408.99$.

1
2
3
4
5
6
7
8
9
10
11
12
13
14
15
16
17
18
19
20
21
22
23
24
25
26
27
28
29
30
31
32
33
34
35
36
37
38
39
40
41
42
43
44
45
46
47
48
49
50
51
52
53
54
55
56
57
58
59
60

Analytical HPLC (Fig. 8) shows a clear difference between the products obtained from the photoreaction of the β polymorph of pure 3-ClCA and the β polymorph of pure 3-BrCA on the one hand and the photoreaction of the $\beta^{(\text{Br})}$ form of the 3-(Cl/Br)CA solid solution (with composition $x_{\text{Cl}} \approx 0.5$) on the other. The product from UV irradiation of the β polymorph of pure 3-ClCA has retention time 11.83 min, whereas the product from UV irradiation of the β polymorph of pure 3-BrCA has retention time 13.69 min (the result from a physical mixture of these two products is shown in Fig. 8a). The product of the photochemical reaction of the $\beta^{(\text{Br})}$ form of the 3-(Cl/Br)CA solid solution gives rise to both of these peaks plus an additional peak with retention time 12.72 min (Fig. 8b). The integrated areas of the peaks at 11.83, 12.72 and 13.69 min are 18.8, 38.3 and 22.7%, respectively, approximately in the 1:2:1 ratio expected for photodimerization in a 1:1 solid solution with a random distribution of 3-ClCA and 3-BrCA molecules (note that the sample analysed also contained unreacted material).

Crystal Structure of the Photodimerization Product

The solid product obtained from UV irradiation (for 60 hrs) of the $\beta^{(\text{Br})}$ form of the 3-(Cl/Br)CA solid solution with $x_{\text{Cl}} \approx 0.5$ was crystallized from acetonitrile and the crystal structure was determined from single-crystal XRD. In the average crystal structure (Fig. 9; triclinic, space group $P1^-$), the asymmetric unit comprises one 3,3'-disubstituted- β -truxinic acid molecule with disorder of Cl and Br at both the 3-position and the 3'-position. The structure also contains acetonitrile, which is disordered, with one molecule of acetonitrile for every two molecules of photodimer. For the specific crystal studied, the refined occupancies of Cl and Br at the 3-position and 3'-position of the β -truxinic acid molecule in the average crystal structure were 0.466(3)/0.534(3) for one site and 0.501(3)/0.499(3) for the other site. These values of occupancy correspond to an overall composition $x_{\text{Cl}} \approx 0.48$, indicating that the crystal has a slight excess of Br over Cl and implying that the 3-bromo-3'-chloro- β -truxinic acid heterodimer cannot be the only product from the reaction, as also deduced above. The crystal structure is isostructural with those reported²⁶ for 3,3'-dibromo- β -truxinic acid and 3,3'-dichloro- β -truxinic acid (which are also solvates, with disordered acetic acid/water sites).

Concluding Remarks

Two γ -type structures (denoted γ and γ') of 3-(Cl/Br)CA solid solutions have been prepared and structurally characterized. The γ form is isostructural with the γ polymorphs of pure 3-ClCA and pure 3-BrCA, which are themselves isostructural. The γ' form is a new structure type within this family of materials, which has so far not been observed for either of the end-members of the family (pure 3-ClCA and pure 3-BrCA).

Two β -type structures (denoted $\beta^{(\text{Cl})}$ and $\beta^{(\text{Br})}$) of 3-(Cl/Br)CA solid solutions have also been prepared and structurally characterized. The $\beta^{(\text{Cl})}$ form is isostructural with the β polymorph of pure 3-ClCA, whereas the $\beta^{(\text{Br})}$ form is isostructural with the β polymorph of pure 3-BrCA. The specific structure type of the solid solution depends on the relative amounts of 3-ClCA and 3-BrCA present in the precursor phase in the preparation procedure. Thus, in materials prepared from molten mixtures of 3-ClCA and 3-BrCA, the $\beta^{(\text{Cl})}$ form is obtained when the mole fraction of 3-ClCA is in the range $x_{\text{Cl}} = 0.75 - 1$ (including the $\beta^{(\text{Cl})}$ structure of pure 3-ClCA as the end-member of this range with $x_{\text{Cl}} = 1$) and the $\beta^{(\text{Br})}$ form is obtained when the mole fraction of 3-ClCA is in the range $x_{\text{Cl}} = 0 - 0.67$ (including the $\beta^{(\text{Br})}$ structure of pure 3-BrCA as the end-member of this range with $x_{\text{Cl}} = 0$). At this stage, we have not yet investigated solid solutions with compositions in the range $x_{\text{Cl}} = 0.67 - 0.75$.

The photoreactivity of the $\beta^{(\text{Br})}$ form of the 3-(Cl/Br)CA solid solution containing a 1:1 molar ratio of 3-ClCA and 3-BrCA has been studied under UV irradiation. Three different products were obtained in the photodimerization reaction: the 3-bromo-3'-chloro- β -truxinic acid heterodimer (denoted {Cl,Br}), the 3,3'-dichloro- β -truxinic acid homodimer (denoted {Cl,Cl}) and the 3,3'-dibromo- β -truxinic acid homodimer (denoted {Br,Br}). The molar ratio of the three photoproducts obtained is approximately 1:2:1 ({Cl,Cl}:{Cl,Br}:{Br,Br}), consistent with the occurrence of a topochemical photodimerization reaction in a solid solution in which there is an essentially random distribution of the reactant molecules 3-ClCA and 3-BrCA.

Experimental

Crystallization from Solution

The samples of 3-CICA and 3-BrCA used in the present work were obtained from Alfa Aesar and solvents were obtained from Fisher. Crystallization was carried out by dissolution in an appropriate solvent (see Table 1), followed by slow evaporation of solvent at ambient temperature. The γ polymorph of pure 3-CICA and the β polymorph of pure 3-CICA were obtained by crystallization from methanol and glacial acetic acid respectively.

A solid solution of 3-CICA and 3-BrCA was prepared by crystallization from a solution containing 3-CICA and 3-BrCA in 1:1 molar ratio in methanol. Colourless block-like crystals were obtained, for which the powder XRD pattern was similar to those of the γ polymorphs of pure 3-CICA and pure 3-BrCA which are isostructural with each other (Fig SI1). Crystallization of 3-CICA and 3-BrCA in a 1:1 molar ratio from acetone produced two types of crystal: colourless thick plates and a small amount of colourless thin needles. Powder XRD showed that the plates were the same phase as that produced from methanol solution, whereas the needles represented a new phase (which is denoted here as the γ' structure).

Crystallization from a solution containing 3-CICA and 3-BrCA in 1:1 molar ratio from glacial acetic acid produced long colourless plates. The powder XRD pattern was similar to that of the β polymorph of pure 3-BrCA (Fig SI2). The product from UV irradiation of these crystals was recrystallized from acetonitrile by slow evaporation, leading to colourless plate-like crystals.

Crystallization from the Melt

Solid solutions of 3-CICA and 3-BrCA were also obtained by crystallization from the molten phase, starting from physical mixtures of solid 3-CICA and solid 3-BrCA in molar ratios corresponding to mole fraction of 3-CICA, $x_{Cl} = 0.17, 0.25, 0.33, 0.50, 0.67, 0.75, 0.80, 0.83$. The physical mixtures were subjected to light grinding to ensure uniform mixing, but care was taken to avoid mechanochemical formation of solid solutions (monitored by powder XRD). To carry out the melting and cooling cycles, the physical mixture was inserted into the DSC instrument (see below) and heated to 200 °C, followed by cooling to ambient temperature to allow crystallization. The

1
2 resultant materials were extracted from the DSC sample holders for analysis by powder XRD and
3 other techniques; in other experiments, a second heating/cooling cycle was carried out in the DSC
4 instrument in order to investigate the thermal behaviour of the resultant materials.
5
6
7

8 9 *Crystal Structure Determination*

10
11
12 Single-crystal XRD data were recorded at either 150 K or ambient temperature using a
13 Nonius Kappa CCD diffractometer (graphite monochromated Mo-K α radiation; $\lambda = 0.71073 \text{ \AA}$) or
14 an Agilent SuperNova Dual Atlas diffractometer [mirror monochromator and either MoK α ($\lambda =$
15 0.71073 \AA) or CuK α ($\lambda = 1.54180 \text{ \AA}$) radiation]. Temperature was controlled using an Oxford
16 Cryosystem cooling apparatus. Crystal structures were solved using direct methods in the
17 program Shelxs-2013³³ and refined using Shelxl-2014.³³ Non-hydrogen atoms were refined with
18 anisotropic displacement parameters. Hydrogen atoms were inserted in idealized positions and
19 refined using a riding model with U_{iso} equal to 1.2 or 1.5 times the value of U_{eq} for the atom to
20 which it is bonded. In some structures, the hydrogen atom of the carboxylic acid group is
21 disordered and modelled with a total occupancy of unity.
22
23
24
25
26
27
28
29
30
31

32 *Powder XRD*

33
34
35 Samples were ground and sandwiched between two pieces of Scotch tape (foil-type sample
36 holder). Powder XRD data were recorded at ambient temperature on a Bruker D8 instrument
37 operating in transmission mode (Ge monochromated CuK α_1 radiation).
38
39
40
41

42 *Differential Scanning Calorimetry*

43
44
45 Differential scanning calorimetry (DSC) data were recorded on a TA Instruments Q100
46 DSC instrument. About 2 – 4 mg of sample was placed in a hermetically sealed pan. Cycles of
47 heating and cooling were studied at a heating/cooling rate of $20 \text{ }^\circ\text{C min}^{-1}$. An equilibration time
48 of 1 min was allowed between heating and cooling cycles.
49
50
51
52

53 *Spectroscopic Analysis*

54
55
56 IR spectra were recorded on a Shimadzu IR Affinity-1 Fourier Transform IR spectrometer.
57 Solution-state ^1H NMR spectra were recorded on a Bruker AM 400 MHz spectrometer, with the
58
59
60

1
2
3 sample dissolved in deuterated methanol (CD₃OD). Electrospray mass spectrometry (ES-MS) was
4
5 carried out using a Waters LCT Premier XE mass spectrometer.
6

7 *Photochemical Reactions*

8
9
10 The reactant material (*ca.* 0.35 g) was ground to a fine powder and spread in a thin layer on
11
12 a glass dish (10 cm diameter). A high-pressure mercury vapour lamp ($\lambda = 300 - 700$ nm) was used
13
14 to irradiate the sample for 60 hrs. The material was agitated every 6 hr to promote uniform
15
16 irradiation. Samples were collected every 6 or 12 hrs to monitor the progress of the reaction by IR
17
18 or solution-state NMR.
19

20 *HPLC*

21
22
23 HPLC was carried out using an Agilent Technology 1200 series liquid chromatograph.
24
25 Chromatographic separation was achieved using RP-HPLC (Phenomenex, Luna C18 (2) column, 5 μ ,
26
27 250 mm \times 4.6 mm). Gradient elution used solvent A (0.1% formic acid in water) and solvent B
28
29 (acetonitrile) with a gradient elution of A:B from 51:49 to 49:51 for 25 min at flow rate 1.0 ml/min.
30
31

32 **Acknowledgements**

33
34
35 We are grateful to Dr Rob Jenkins for assistance with HPLC experiments. We thank the
36
37 Kingdom of Saudi Arabia (M.A.K.) and Cardiff University for financial and material support.
38
39
40
41
42
43
44

45 **Supporting Information**

46
47
48 PXRD Figures SI1 and SI2.
49
50
51
52
53
54
55
56
57
58
59
60

Table 1 Summary of preparation methods for 3-(Cl/Br)CA solid solutions and the pure materials 3-ClCA ($x_{Cl} = 1$) and 3-BrCA ($x_{Cl} = 0$)

Stoichiometry (x_{Cl})	Structure Type	Molecular Conformation	Preparation Procedure	Reference
0 → 1	$\beta^{(Br)}$ ($x_{Cl} = 0 \rightarrow 0.67$) $\beta^{(Cl)}$ ($x_{Cl} = 0.75 \rightarrow 1$)	<i>syn</i> <i>anti</i>	Crystallization from molten phase	This work
0.5	$\beta^{(Br)}$	<i>syn</i>	Crystallization from glacial acetic acid	This work
0.5	γ	<i>anti</i>	Crystallization from methanol	This work
0.5	γ (plate crystals) γ' (needle crystals)	<i>anti</i> <i>anti</i>	Crystallization from acetone	This work
0	$\beta^{(Br)}$	<i>syn</i>	See ref. 26	26
0	γ	<i>anti</i>	See ref. 28	28
1	$\beta^{(Cl)}$	<i>anti</i>	See ref. 26	26
1	γ	<i>anti</i>	See ref. 27	27

Table 2 Crystallographic data for known polymorphs of pure 3-ClCA and pure 3-BrCA.

Compound	3-ClCA	3-BrCA	3-ClCA	3-BrCA
Polymorph	β	β	γ	γ
Reference	26	26	27	28
Space Group	$\bar{P}1$	$C2/c$	$P2_1/a$	$P2_1/a$
$a / \text{\AA}$	8.618(4)	19.191(6)	12.400(1)	12.389(2)
$b / \text{\AA}$	13.627(5)	3.9879(3)	4.9560(4)	4.933(5)
$c / \text{\AA}$	3.909(1)	24.798(7)	13.943(1)	14.411(2)
$\alpha / ^\circ$	106.77(3)	90	90	90
$\beta / ^\circ$	96.26(3)	113.05(2)	94.265(3)	95.426(5)
$\gamma / ^\circ$	75.71(3)	90	90	90
Temp / K	295	295	293	293

Table 3 Crystallographic Data

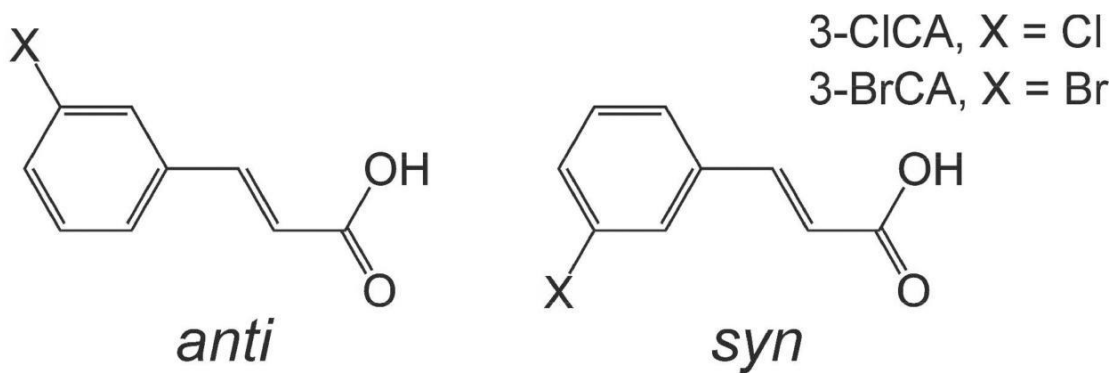
	γ Form of 3-(Cl/Br)CA Solid Solution ($x_{Cl} = 0.56$)	γ' Form of 3-(Cl/Br)CA Solid Solution ($x_{Cl} = 0.61$)	$\beta^{(Br)}$ Form of 3-(Cl/Br)CA Solid Solution ($x_{Cl} = 0.51$)	Acetonitrile Solvate of Recrystallized Photoproduct from the $\beta^{(Br)}$ Form of the 3-(Cl/Br)CA Solid Solution ($x_{Cl} \approx 0.48$)
Formula	$C_9H_7Cl_{0.44}O_{0.56}Br_2$	$C_9H_7Cl_{0.39}O_{0.61}Br_2$	$C_9H_7Cl_{0.49}O_{0.51}Br_2$	$C_{19}H_{15.5}Br_{0.97}Cl_{1.03}N_{0.5}O_4$
FW	202.38	199.93	204.38	428.62
T (K)	150(2)	293(2)	150(2)	296(2)
λ (Å)	0.71073	1.54184	0.71073	0.71073
System	Monoclinic	Monoclinic	Monoclinic	Triclinic
Space group	$P2_1/a$	$P2_1/n$	$C2/c$	$P1^-$
a (Å)	12.2786(9)	4.9671(5)	19.0797(10)	8.5769(6)
b (Å)	4.9068(2)	28.125(3)	3.86490(10)	14.2022(10)
c (Å)	14.1487(10)	6.1401(7)	24.4818(12)	8.1299(5)
α (°)	90	90	90	103.985(5)
β (°)	95.242(2)	91.259(9)	111.944(2)	102.631(5)
γ (°)	90	90	90	79.990(6)
V (Å ³)	848.87(9)	857.56(17)	1674.52(13)	930.02(11)
Z	4	4	8	2
Occupancy of Cl / Br	0.556(4) / 0.444(4)	0.610(8) / 0.390(8)	0.510(4) / 0.490(4)	0.466(3) / 0.534(3) 0.501(3) / 0.499(3)
σ (calc) (Mg/m ³)	1.584	1.549	1.621	1.531
μ (mm ⁻¹)	2.356	4.585	2.589	2.305
$F(000)$	408	404	823	433
Crystal size (mm ³)	0.30 × 0.25 × 0.07	0.46 × 0.07 × 0.04	0.39 × 0.2 × 0.04	0.45 × 0.30 × 0.09
Wavelength (Å)	0.71073	1.54180	0.71073	0.71073
Collected	3358	2928	4414	8241
Independent	1927	1662	1879	4374
R (int)	0.0348	0.0374	0.0309	0.0214
GOF on F^2	1.052	1.078	1.072	1.020
R_1 [$I > 2\sigma(I)$]	0.0407	0.0704	0.0288	0.0440
wR ₂	0.0817	0.1832	0.0648	0.0811
R_1 (all data)	0.0617	0.0829	0.0338	0.0827
wR ₂ (all data)	0.0888	0.1908	0.0678	0.0935

References

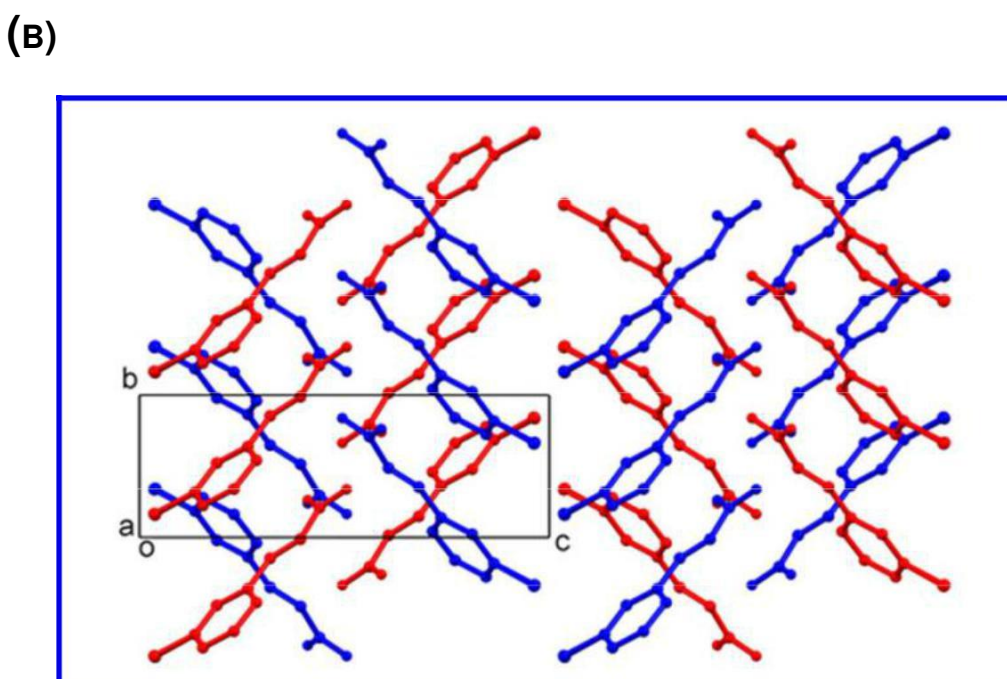
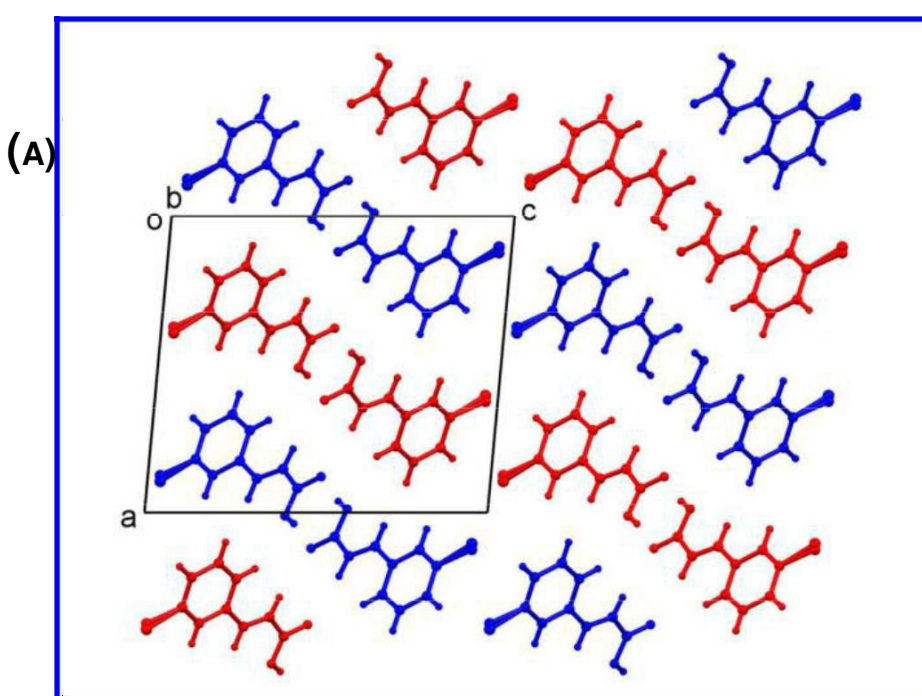
- (1) Kohlschutter, V.; Tuscher, J. L. *Z. Anorg. Allg. Chem.* **1920**, *111*, 193-236.
- (2) Cohen, M. D.; Schmidt, G. M. J. *J. Chem. Soc.* **1964**, 1996-2000.
- (3) Cohen, M. D.; Schmidt, G. M. J.; Sonntag, F. I. *J. Chem. Soc.* **1964**, 2000-2013.
- (4) Schmidt, G. M. J. *J. Chem. Soc.* **1964**, 2014-2021.
- (5) Cohen, M. D. *Pure Appl. Chem.* **1964**, *9*, 567-574.
- (6) Hirshfield, F. L.; Schmidt, G. M. J. *J. Polym. Sci.* **1964**, *2*, 2181-2190.
- (7) Schmidt, G. M. J. In *Photochemistry of the Solid State, Reactivity of the Photoexcited Molecule*, Interscience, New York, **1967**, pp 227-284.
- (8) Schmidt, G. M. J. *Pure Appl. Chem.* **1971**, *27*, 647-678.
- (9) Thomas, J. M. *Phil. Trans. Royal Soc. A* **1974**, *277*, 251-287.
- (10) Cohen, M. D. *Angew. Chem.* **1975**, *87*, 439-447.
- (11) Thomas, J. M. *Pure Appl. Chem.* **1979**, *51*, 1065-1082.
- (12) Nakanishi, H.; Jones, W.; Thomas, J. M.; Hursthouse, M. B.; Motevalli, M. *J. Phys. Chem.* **1981**, *85*, 3636-3642.
- (13) Hasegawa, M. *Pure Appl. Chem.* **1986**, *58*, 1179-1188.
- (14) Harris, K. D. M.; Thomas, J. M.; Williams, D. J. *Chem. Soc. Faraday Trans.* **1991**, *87*, 325-331.
- (15) Enkelmann, V.; Wegner, G.; Novak, K.; Wagener, K. B. *J. Am. Chem. Soc.* **1993**, *115*, 10390-10391.
- (16) Guo, F.; Martí-Rujas, J.; Pan, Z.; Hughes, C. E.; Harris, K. D. M. *J. Phys. Chem. C* **2008**, *112*, 19793-19796.
- (17) Mustafa, A. *Chem. Rev.* **1952**, *51*, 1-23.
- (18) Desiraju, G. R.; Sharma, C. V. K. M. *J. Chem. Soc. Chem. Commun.* **1991**, 1239-1241.
- (19) Sharma, C. V. K.; Panneerselvam, K.; Shimoni, L.; Katz, H.; Carrell, H. L.; Desiraju, G. R. *Chem. Mater.* **1994**, *6*, 1282-1292.
- (20) Hung, J. D.; Lahav, M.; Luwisch, M.; Schmidt, G. M. J. *J. Chem. Soc. Perkin Trans. 2* **1972**, *10*, 585-599.
- (21) Cohen, M. D.; Cohen, R.; Lahav, M.; Nie, P. L. *J. Chem. Soc. Perkin Trans. 2* **1973**, 1095-1100.
- (22) Elgavi, A.; Green, B. S.; Schmidt, G. M. J. *J. Am. Chem. Soc.* **1973**, *95*, 2058-2059.
- (23) Cohen, M. D.; Cohen, R. *J. Chem. Soc. Perkin Trans. 2* **1976**, 1731-1735.
- (24) Theocharis, C. R.; Desiraju, G. R.; Jones, W. *J. Am. Chem. Soc.* **1984**, *106*, 3606-3609.
- (25) Bucar, D.-K.; Sen, A.; Mariappan, S. V. S.; MacGillivray, L. R. *Chem. Commun.* **2012**, *48*, 1790-1792.
- (26) Kanao, S.; Kashino, S.; Haisa, M. *Acta Cryst. Sect. C* **1990**, *46*, 2436-2438.
- (27) Kariuki, B. M.; Zin, D. M. S.; Tremayne, M.; Harris, K. D. M. *Chem. Mater.* **1996**, *8*, 565-569.
- (28) Ahn, S.; Harris, K. D. M.; Kariuki, B. M.; Zin, D. M. S. *J. Solid State Chem.* **2001**, *156*, 10-15.
- (29) Hachula, B.; Jablonska-Czapla, M.; Flakus, H. T.; Nowak, M.; Kusz, J. *Spectrochim Acta A* **2015**, *125*, 592-597.
- (30) Vegard, L. *Z. Phys.* **1921**, *5*, 17-26.
- (31) Denton, A. R.; Ashcroft, N. W. *Phys. Rev. A* **1991**, *43*, 3161-3164.
- (32) Khoj, M. A.; Hughes, C. E.; Harris, K. D. M.; Kariuki, B. M. *Cryst. Growth Des.* **2013**, *13*, 4110-4117.
- (33) Sheldrick, G. M. *Acta Crystallogr. Sect. A* **2008**, *64*, 112-122.

1
2
3
4
5
6
7
8
9
10
11
12
13
14
15
16
17
18
19
20
21
22
23
24
25
26
27
28
29
30
31
32
33
34
35
36
37
38
39
40
41
42
43
44
45
46
47
48
49
50
51
52
53
54
55
56
57
58
59
60

Figures



Scheme 1. Molecular structures of 3-CICA and 3-BrCA, and definition of the molecular conformations *anti* and *syn* discussed in the text.



48
49
50
51
52
53
54
55
56
57
58
59
60

Figure 1: Crystal structure of the γ form of the 3-(Cl/Br)CA solid solution (with $x_{Cl} \approx 0.56$): (a) viewed along the b -axis (the stacking axis), and (b) viewed along the c -axis (illustrating the herring-bone arrangement of hydrogen-bonded pairs of molecules within a given layer parallel to the bc -plane). In both (a) and (b), molecules in adjacent layers are shown in red and blue. All hydrogen atoms in (b) and one component of the disordered carboxylic acid hydrogen in (a) are omitted for clarity.

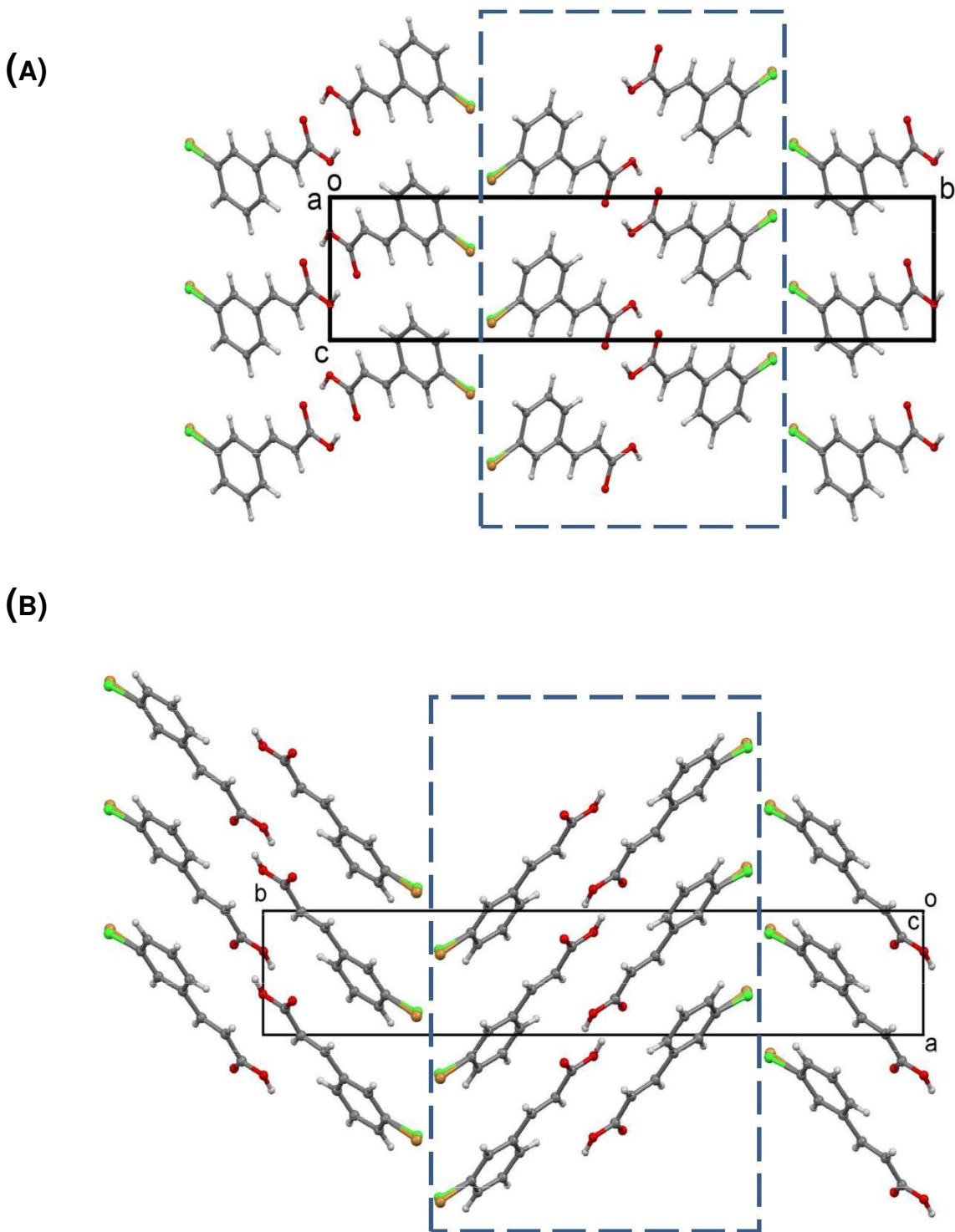


Figure 2: Crystal structure of the γ' form of the 3-(Cl/Br)CA solid solutions (structure determined for a crystal with $x_{\text{Cl}} \approx 0.61$): (a) viewed along the a -axis (the stacking axis), and (b) viewed along the c -axis. The Cl and Br atoms at the disordered Cl/Br site are shown in green and brown respectively. The dashed boxes indicated the regions (parallel to the ac -plane) defined as “slabs” in the text.

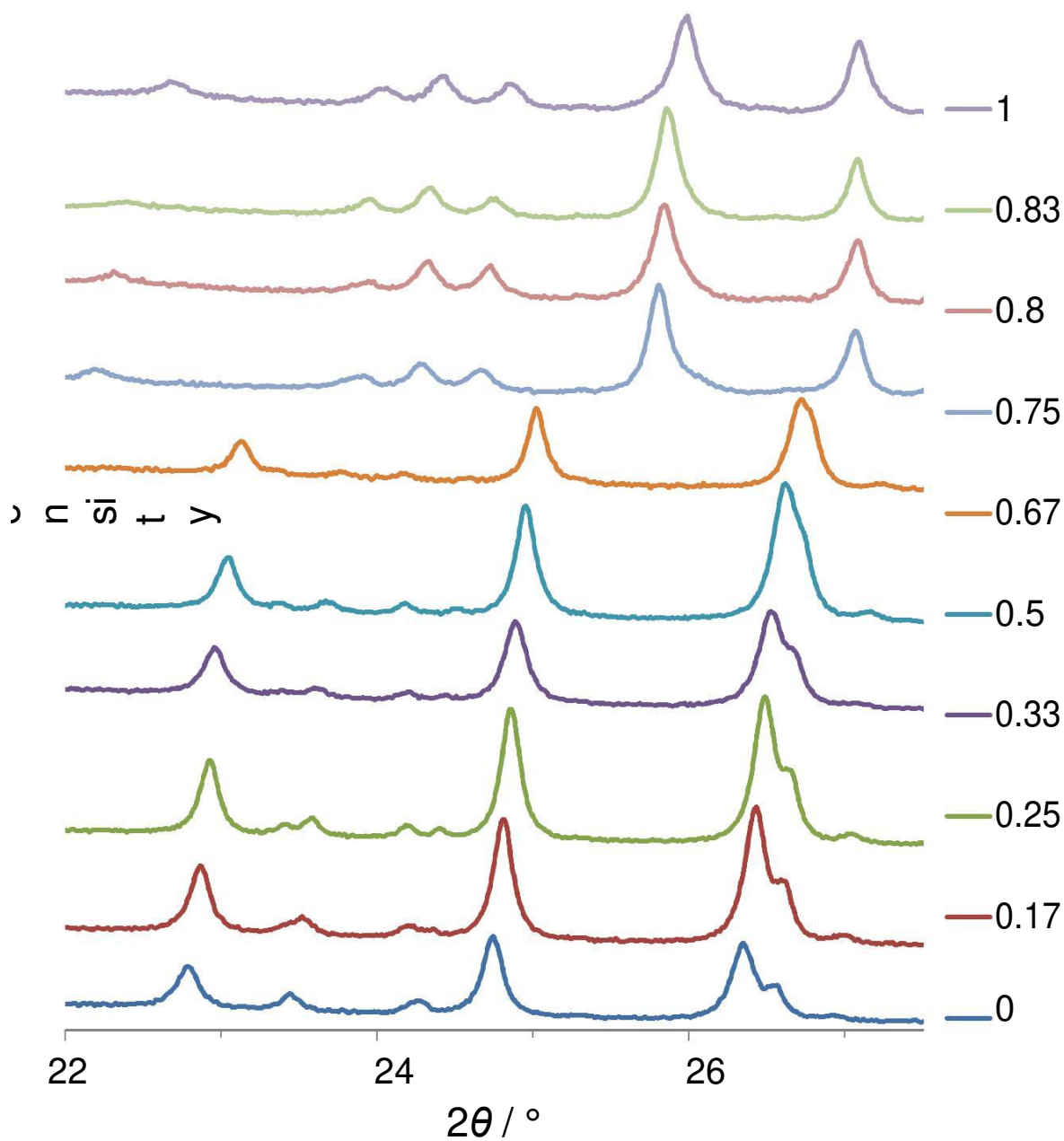


Figure 3: Selected region of the powder XRD patterns for the β polymorph of pure 3-BrCA ($x_{\text{Cl}} = 0$), the β polymorph of pure 3-ClCA ($x_{\text{Cl}} = 1$), and the 3-(Cl/Br)CA solid solutions with the $\beta^{(\text{Br})}$ structure type ($x_{\text{Cl}} = 0.17 - 0.67$) and $\beta^{(\text{Cl})}$ structure type ($x_{\text{Cl}} = 0.75 - 0.83$).

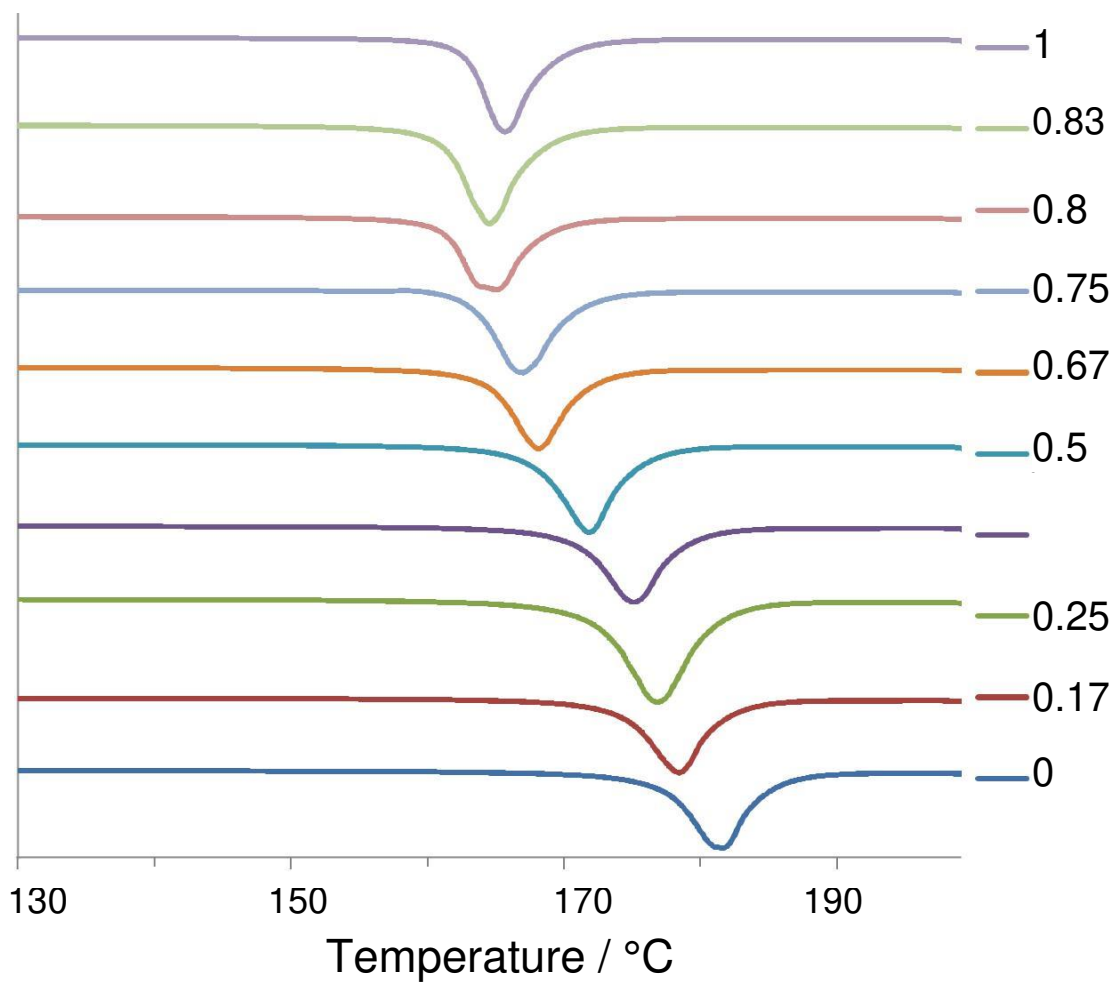
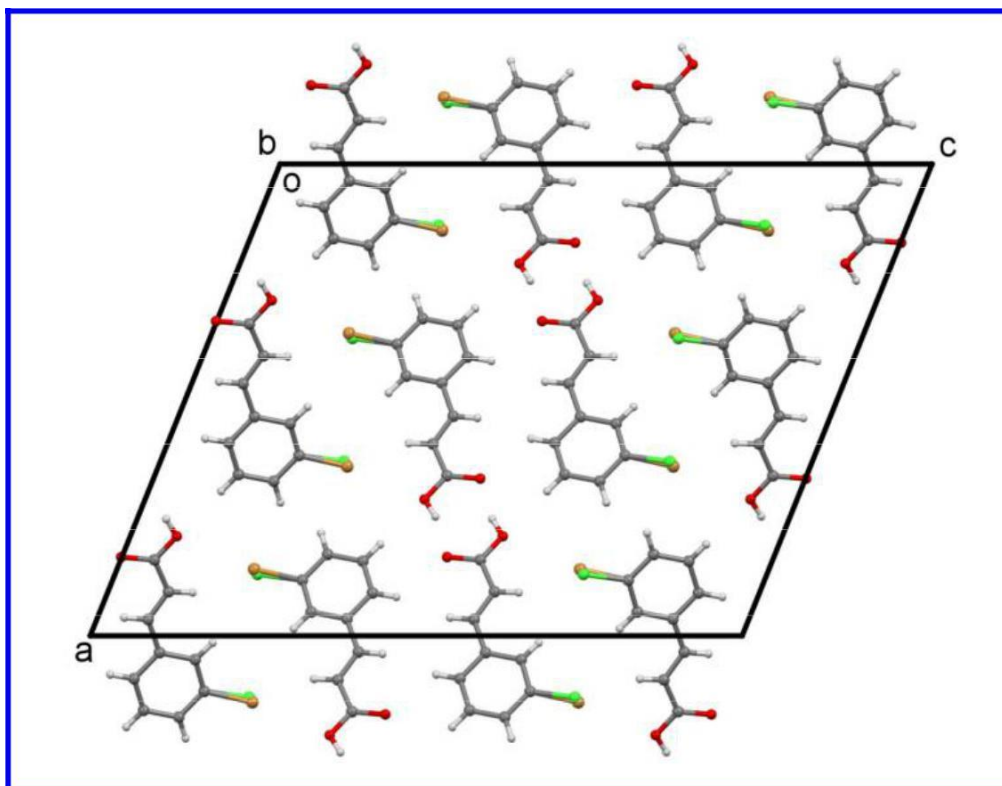


Figure 4: DSC data recorded in the heating cycle for the β polymorph of pure 3-BrCA ($x_{Cl} = 0$), the β polymorph of pure 3-ClCA ($x_{Cl} = 1$), and the 3-(Cl/Br)CA solid solutions with the $\beta^{(Br)}$ structure type ($x_{Cl} = 0.17 - 0.75$) and $\beta^{(Cl)}$ structure type ($x_{Cl} = 0.80 - 0.83$).

(A)



(B)

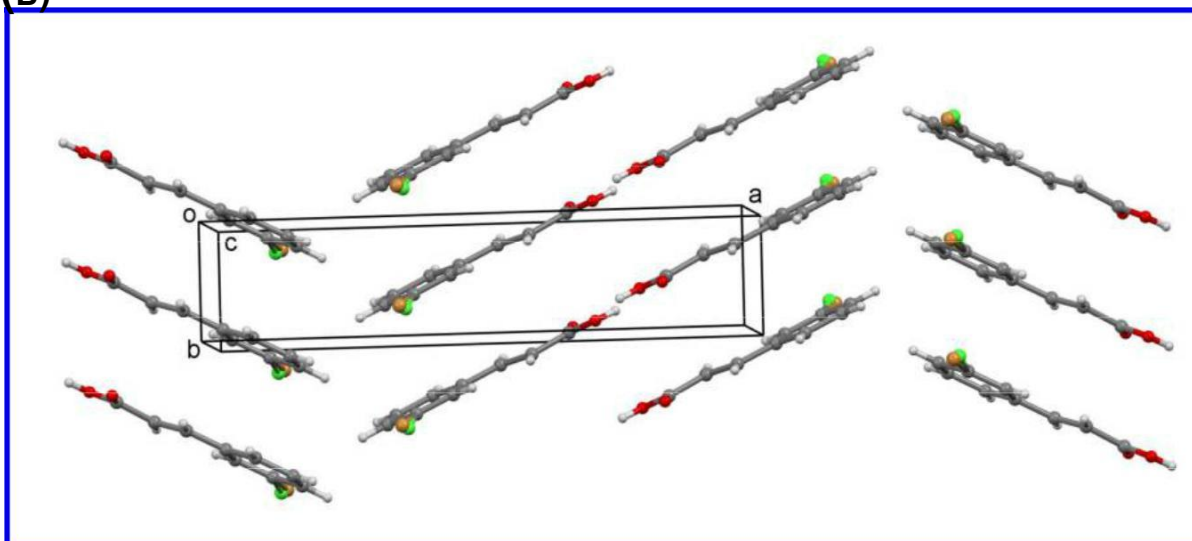
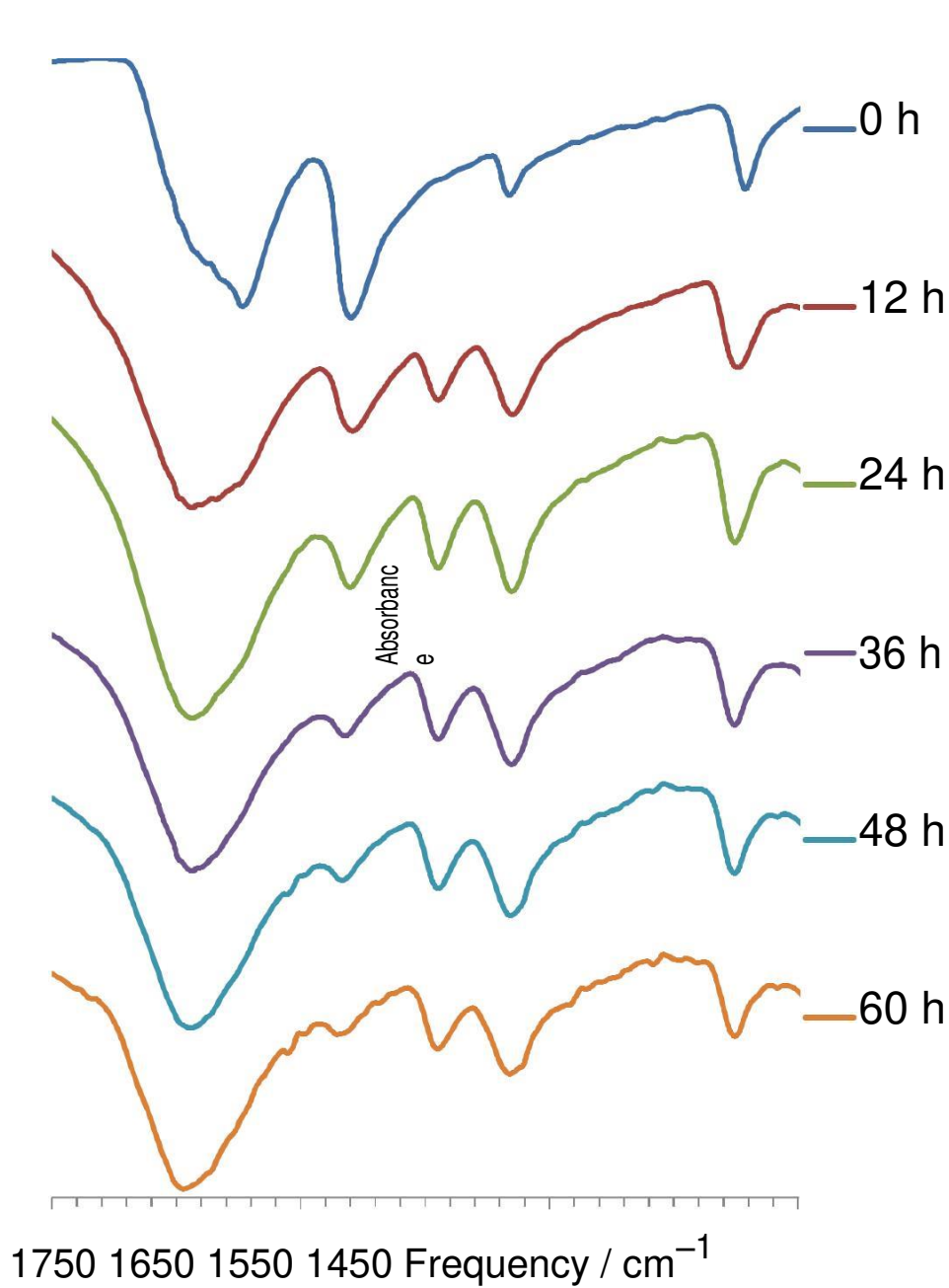
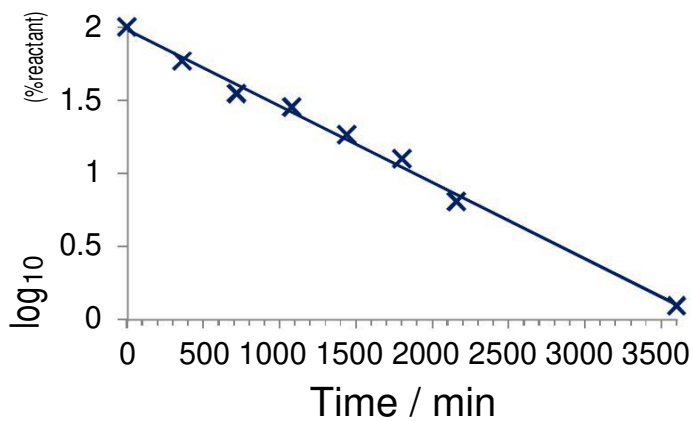
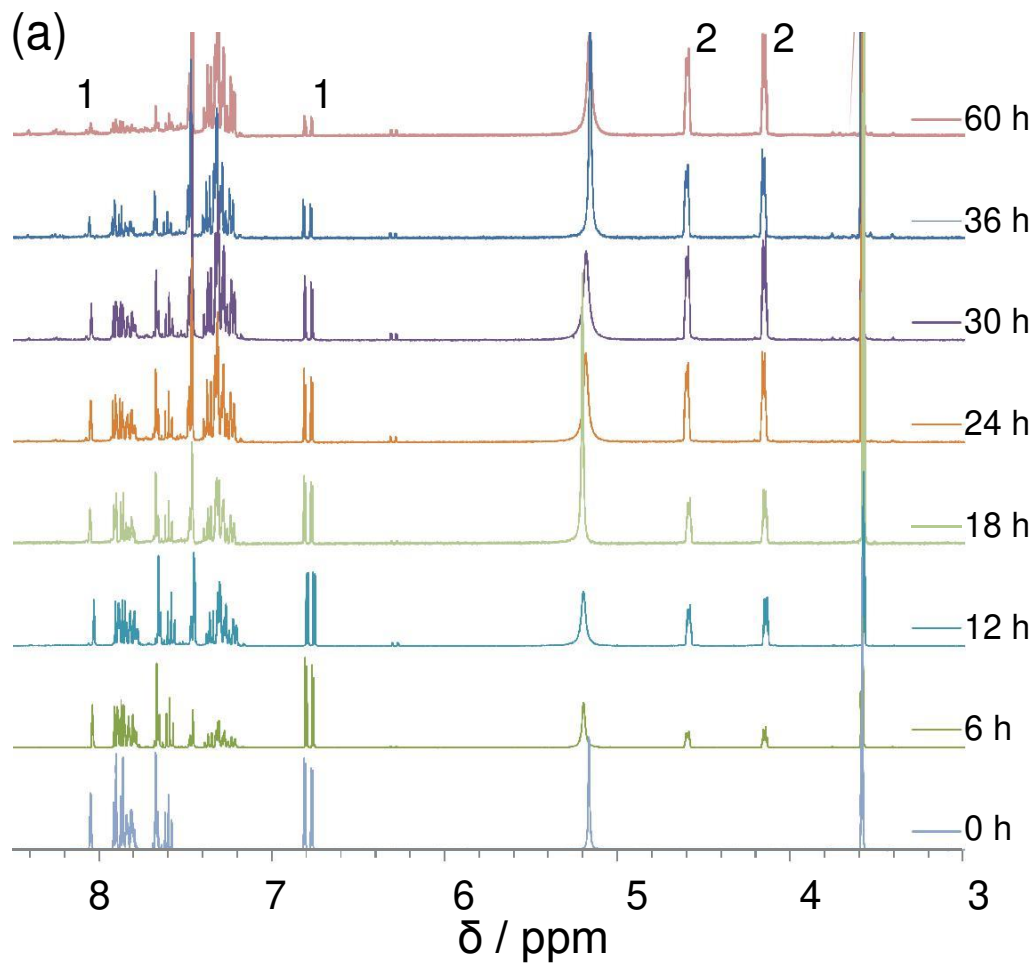


Figure 5: Crystal structure of the $\beta^{(\text{Br})}$ form of the 3-(Cl/Br)CA solid solution (with composition $x_{\text{Cl}} \approx 0.51$): (a) viewed along the b -axis (the stacking axis), and (b) viewed approximately along the c -axis (showing a single layer of stacked molecules). The Cl and Br atoms at the disordered Cl/Br site are shown in green and brown respectively. One component of the disordered hydrogen atom of the carboxylic acid group is shown.



45
46
47
48
49
50
51
52
53
54
55
56
57
58
59
60

Figure 6: FTIR data recorded *ex-situ* for samples extracted at different times (indicated at the right side) during UV irradiation of a powder sample of the $\beta^{(\text{Br})}$ form of the 3-(Cl/Br)CA solid solution with composition $x_{\text{Cl}} \approx 0.5$.



52
53
54
55
56
57
58
59
60

Figure 7: (a) Solution-state ^1H NMR spectra of samples extracted at different times during UV irradiation of the $\beta^{(\text{Br})}$ form of the 3-(Cl/Br)CA solid solution with composition $x_{\text{Cl}} \approx 0.5$. (b) Plot of $\log_{10}(\text{reactant}\%)$ versus time, established from the solution-state ^1H NMR spectra shown in (a).

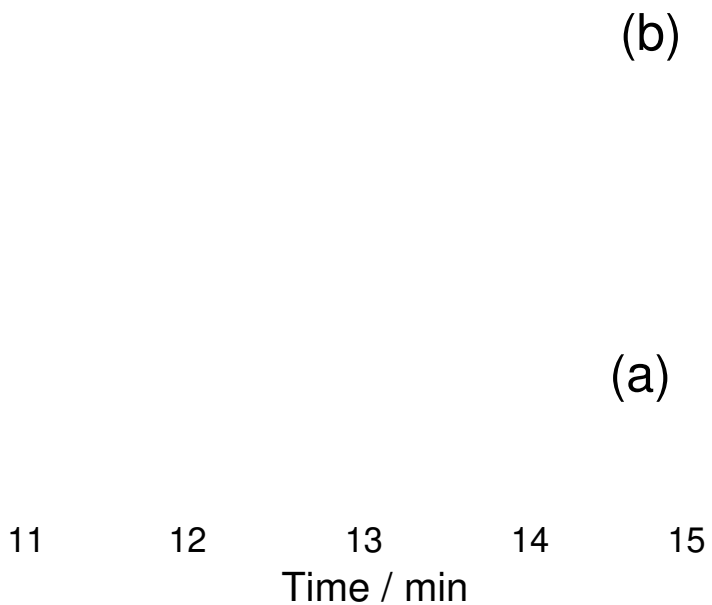


Figure 8: HPLC data for: (a) a physical mixture of the solidphotodimers obtained from UV irradiation of the β polymorph of pure 3-ClCA and the β polymorph of pure 3-BrCA, and (b) the photoproduct obtained from UV irradiation of the 3-(Cl/Br)CA solid solution with the $\beta^{(\text{Br})}$ structure type and composition $x_{\text{Cl}} \approx 0.5$.

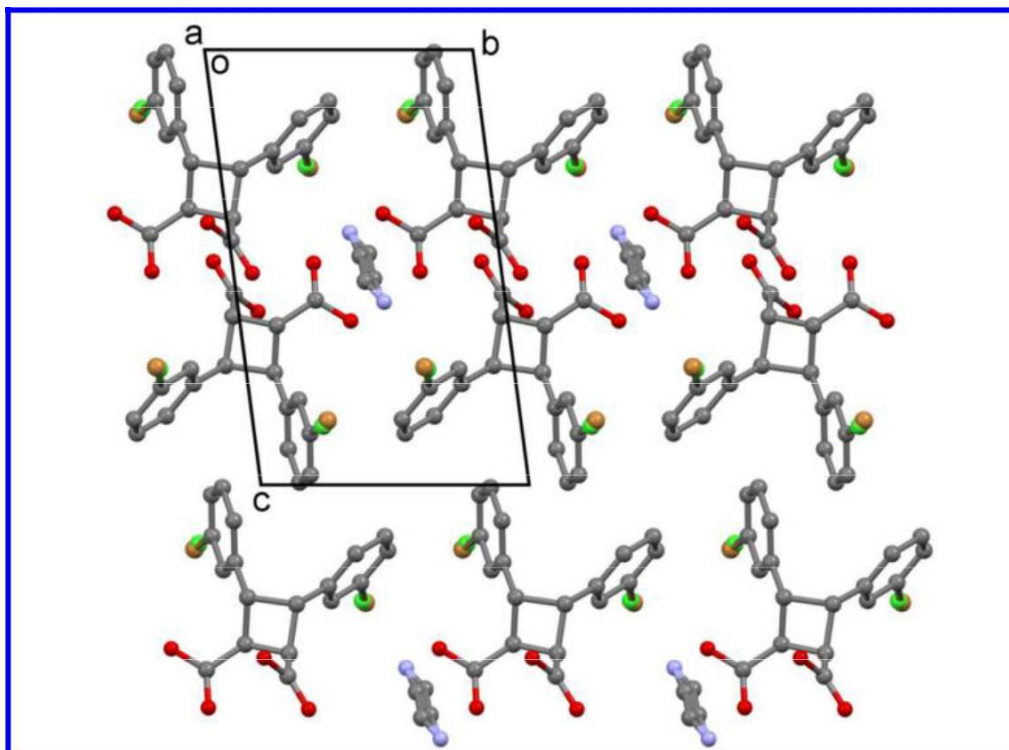
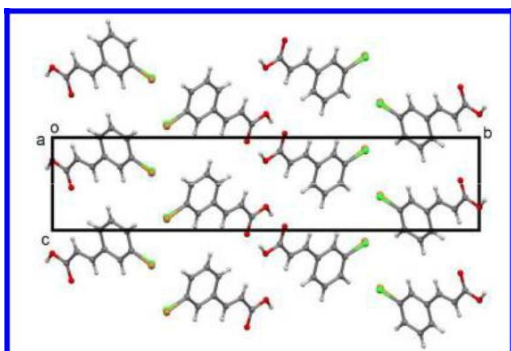


Fig 9: Crystal structure of the photoproduct obtained from UV irradiation of the 3-(Cl/Br)CA solid solution with the $\beta^{(\text{Br})}$ structure type and composition $x_{\text{Cl}} \approx 0.48$, following recrystallization from acetonitrile. The Cl and Br atoms at the disordered Cl/Br site are shown in green and brown respectively. The crystal is an acetonitrile solvate containing one disordered acetonitrile molecule for every two molecules of photodimer. Hydrogen atoms are omitted for clarity.

1
2
3 **For Table of Contents Use Only**
4
5
6
7

8 **Structural diversity of solid solutions formed between 3-chloro-*TRANS*-cinnamic**
9 **acid and 3-bromo-*TRANS*-cinnamic acid**
10
11

12 Manal A. Khoj, Colan E. Hughes, Kenneth D. M. Harris* and Benson M. Kariuki*
13
14
15



28
29
30 Studies of the formation and structural properties of solid solutions containing 3-chloro-*trans*-
31 cinnamic acid and 3-bromo-*trans*-cinnamic acid reveal two β -type structures and two γ -type
32 structures, one of which is not observed for the pure phases of 3-chloro-*trans*-cinnamic acid or 3-
33 bromo-*trans*-cinnamic acid. Analysis of product distributions following UV irradiation is
34 consistent with a random distribution of the two types of molecule in the solid solutions.
35
36
37
38
39
40
41
42
43
44
45
46
47
48
49
50
51
52
53
54
55
56
57
58
59
60